

Published in final edited form as:

*J Proteome Res.* 2013 March 1; 12(3): 1134–1141. doi:10.1021/pr301107x.

## Enrichment of plasma membrane proteins using nanoparticle pellicles: comparison between silica and higher density nanoparticles

Waeowalee Choksawangkarn<sup>#,1</sup>, Sung-Kyoung Kim<sup>#,1</sup>, Joe R. Cannon<sup>1</sup>, Nathan J. Edwards<sup>2</sup>, Sang Bok Lee<sup>1,3</sup>, and Catherine Fenselau<sup>1</sup>

<sup>1</sup>Department of Chemistry and Biochemistry, University of Maryland, College Park, Maryland 20742

<sup>2</sup>Department of Biochemistry and Molecular & Cellular Biology, Georgetown University Medical Center, Washington DC 20057

<sup>3</sup>Graduate School of Nanoscience and Technology (WCU), Korea Advanced Institute of Science and Technology, Daejeon, Korea

### Abstract

Proteomic and other characterization of plasma membrane proteins is made difficult by their low abundance, hydrophobicity, frequent carboxylation and dynamic population. We and others have proposed that underrepresentation in LC-MS/MS analysis can be partially compensated by enriching the plasma membrane and its proteins using cationic nanoparticle pellicles. The nanoparticles increase the density of plasma membrane sheets and thus enhance separation by centrifugation from other lysed cellular components. Herein we test the hypothesis that the use of nanoparticles with increased densities can provide enhanced enrichment of plasma membrane proteins for proteomic analysis. Multiple myeloma cells were grown and coated in suspension with three different pellicles of three different densities and both pellicle coated and uncoated suspensions analyzed by high-throughput LC-MS/MS. Enrichment was evaluated by the total number and the spectral counts of identified plasma membrane proteins.

### Keywords

Plasma membrane; nanoparticles; pellicle enrichment; proteomics; spectral counting

### Introduction

Thirty percent of the human genome is predicted to express plasma membrane proteins (1), which play critical roles in communications and interactions between cells and their environment. Reflecting these functions, proteins in the plasma membrane and cell surface are reported to account for more than 60% of the drug targets currently under development (2,3). However, they are present in the cell in low abundance, on average, and are characterized by their hydrophobicity and glycosylation. Consequently they are usually underrepresented in untargeted biochemical and proteomic studies. Several strategies have been proposed to enrich plasma membrane proteins that take advantage of accessibility to the exterior cell surface. These include affinity capture using immobilized antibodies or lectins (4) and the alkylation of reactive amino acid residues or oxidized carbohydrate

<sup>#</sup>These two authors contributed equally to the study.

moieties with reagents linked to biotin (5-7) to isolate cell surface proteins and glycoproteins. We have undertaken to enrich the entire plasma membrane to analyze integral proteins and proteins from both the inner and outer surfaces, using pellicles formed with cationic nanoparticles. We are also optimizing a proteomic workflow to provide proteolysis of highly hydrophobic proteins (8).

The use of cationic colloidal silica was first introduced by Jacobson and coworkers (9,10) to increase the density of the plasma membrane and enhance its separation by centrifugation from the rest of the lysed cell. Jacobson and many subsequent researchers have synthesized alumina-coated silica nanoparticles to achieve a cationic surface at physiological pH, which is attracted electrostatically to the anionic cell surface. (Alumina functional groups have isoelectric points (pI) around pH 8.) A nanostructure is defined as having at least one dimension between 1 and 100 nm. The reported average diameter of Jacobson's nanoparticles is reported to be around 50 nm (10-12). A related, commercial product has also been used, an aluminosilicate colloid sold as Ludox, with a diameter close to 20 nm (12-18).

Two distinct applications of pellicles have been reported through the last thirty years--enrichment of the plasma membrane and associated proteins from cells grown in suspension or isolated in suspension from blood or tissue (17), and use of the heavy silica nanoparticles to fracture the apical from the basolateral plasma membrane domains in luminal cells in microvasculature (19) or adherent cells in culture (15). The present study addresses the enrichment of plasma membrane proteins from a multiple myeloma cell line cultured and coated in suspension and supports our on-going studies of plasma membrane proteins in myeloid derived suppressor cells isolated from mouse blood. Prior reports of work with suspended mammalian cells have assessed the enrichment of plasma membrane proteins by Western blotting of marker proteins, most frequently  $\text{Na}^+\text{-K}^+$  ATPase. Enrichments of  $\text{Na}^+\text{-K}^+$  ATPase from cells coated in suspension have been reported between 15-fold and 20-fold (14,17,20).

Recently, we (14,15) and other laboratories (for example, 3,12,16-17, 20-25) have integrated the use of nanoparticle pellicles into high throughput proteomic workflows. This advanced technology allows broad evaluation of enrichment, based on the identification of large numbers of proteins and their classification as plasma membrane, transmembrane, cell surface, cytoskeletal, etc. using Gene Ontology (GO) cellular component annotations. In these experiments enrichment can be evaluated by reporting cohorts such as the plasma membrane proteins as a percent of total proteins identified. Plasma membrane proteins characterized in this manner from suspended mammalian cells are previously reported to comprise between 18 and 42 % of total proteins identified (14,17,20,22). These estimates are uncertain for several reasons. First, experimentally-based assignments of cellular locations are incomplete, and computationally-based annotations are prone to false positives and false negatives. Different data-resources, notably, UniProt and the Gene Ontology (GO) provide similar, but distinct, cellular location namespaces and annotations which may, or may not, apply the same evidence to determine cellular location — in some cases, these data-resources even cite each other! In addition, many cellular proteins move dynamically through the plasma membrane, but are annotated as belonging to other parts of the cell (3, 26). Often these proteomic studies do not provide an analysis of the whole cell lysate or other control sample, thus obscuring the actual effect of the pellicle treatment. Lastly, counting identified proteins with a particular GO annotation does not reflect qualitative enrichment of different proteins in the plasma membrane fraction, and both spectral counting (23) and isotope labeling (22) have been employed to augment the protein counting approach.

Given the real need for effective enrichment of the plasma membrane, can more effective pellicle nanostructures be designed? In the present work we test the hypothesis that enrichment of the plasma membrane of multiple myeloma cells can be enhanced by the use of nanoparticles with higher density.

## Materials and Methods

### Materials

Human multiple myeloma RPMI 8226 and RPMI 1640 medium were purchased from American Type Culture Collection (Manassas, VA). Fetal bovine serum was obtained from Atlanta Biologicals (Lawrenceville, GA). Poly(acrylic acid) (MW=100,000), Penicillin-Streptomycin solution, mouse monoclonal anti- $\text{Na}^+\text{-K}^+$  ATPase ( $\alpha$ -subunit) primary antibody, alkaline phosphatase-conjugated goat anti-mouse IgG, BCIP®/NBT solution, Tween-20, D-sorbitol, 2-(N-morpholino)ethanesulfonic acid (MES), NaCl, imidazole, protease inhibitor cocktail solution,  $\text{Na}_2\text{CO}_3$ , KCl,  $\text{NH}_4\text{HCO}_3$ , urea, dithiothreitol (DTT), iodoacetamide, glutaraldehyde, Tris-HCl,  $\beta$ -mercaptoethanol, and SDS were purchased from Sigma-Aldrich (St. Louis, MO). Criterion Tris-HCl precast gels, Tris-glycine-SDS buffer, molecular weight standards, and RC DC protein assay kit were purchased from Bio-Rad (Hercules, CA). Endoproteinase Lys-C and trypsin were purchased from Promega (Madison, WI). PVDF membrane was purchased from Millipore (Billerica, MA). Optima LC/MS grade acetonitrile, formic acid, trifluoroacetic acid, Pierce® C18 spin columns were purchased from Fisher Scientific (Pittsburgh PA). Pierce® C18 spin columns were purchased from Fisher Scientific. For nanoparticle synthesis, ferric chloride hexahydrate ( $\text{FeCl}_3 \cdot 6\text{H}_2\text{O}$ , 97.0-102.0%) was obtained from Alfa Aesar (Ward Hill MA,). Propylene glycol (JT Baker, NJ, USA) and sodium acetate (ACS reagent grade) were obtained from Fisher Scientific. Aluminum nitrate nonahydrate ( $\text{Al}(\text{NO}_3)_3 \cdot 9\text{H}_2\text{O}$ , 98%) and Potassium nitrate ( $\text{K}(\text{NO}_3)$ , 99.0%) were purchased from Sigma-Aldrich. Deionized water was obtained by a Milli-Q A10 system and was used for all the experiments.

$\text{SiO}_2/\text{Al}_2\text{O}_3$  nanoparticles were kindly provided by Prof. Donna Beer Stolz, University of Pittsburg (10). LUDOX-CL cationic colloidal silica (aluminosilicate) was purchased from Sigma-Aldrich.

### Synthesis of $\text{Fe}_3\text{O}_4$ nanoparticles coated with $\text{Al}_2\text{O}_3$

Iron oxide particles have been synthesized by a polyol method (27). Briefly, 0.005 M  $\text{FeCl}_3 \cdot 6\text{H}_2\text{O}$  and 0.0015 M sodium acetate were dissolved in 25 ml propylene glycol. Five hundred microliters water was added to the polyol medium for hydrolysis reaction, which were refluxed for 12 hours in a 100 ml roundbottomed flask fitted with a condenser held at room temperature. The resulting particles were washed with water using centrifuge, followed by immersing into 10 ml of 0.01 M  $\text{Al}(\text{NO}_3)_3/0.1$  M  $\text{K}(\text{NO}_3)$  aqueous solution for 12 hours with gentle rocking at room temperature. The aluminacoated particles were dispersed in water before using in plasma membrane enrichment experiment. The physical characteristics of the particles were analyzed by a SU-70 Field Emission SEM (Hitachi High Technologies America, Pleasanton CA), a JEM-2100F Field Emission TEM (JEOL USA, Peabody MA) operating at 200 kV with scanning TEM capability, an Oxford energy dispersive x-ray (EDX) spectrometer, and a Zetasizer Nano ZS90 particle analyzer (Malvern Instruments Ltd., Worcestershire UK).

### Cell Culture and Pellicle Coating

Human multiple myeloma RPMI 8226 cells were cultured in RPMI 1640 medium supplemented with 10% fetal bovine serum and antibiotics at 37 °C and 5%  $\text{CO}_2$ , and harvested at confluence. Although different harvests were used to evaluate the different

pellicles, all preparations were made in the same manner, to the best of our ability. Approximately,  $6 \times 10^7$  cells in suspension were collected at 900 xg for 5 min, and washed with plasma membrane coating buffer A (PMCBA, 800 mM sorbitol, 20 mM MES, 150 mM NaCl, pH 5.3). The cells were coated with cationic nanoparticles, including  $\text{SiO}_2/\text{Al}_2\text{O}_3$ , LUDOX-CL  $\text{SiO}_2$  (comprising aluminosilicate), and  $\text{Fe}_3\text{O}_4/\text{Al}_2\text{O}_3$  nanoparticles, following our published procedures with slight modifications (8,14). In brief, the cells resuspended in PMCBA were placed dropwise into 10% (w/v) cationic nanoparticle solutions and rocked gently at 4 °C for 15 min. The nanoparticle-coated cells were added dropwise to 10 mg/mL poly(acrylic acid) in PMCBA, pH 6.0-6.5, and incubated at 4 °C for 15 min with gently rocking. The poly(acrylic acid) cross-linked cells were sedimented and washed with PMCBA to remove unbound poly(acrylic acid). The cells were incubated in 2.5 mM imidazole with a protease inhibitor cocktail, at 4 °C for 30 min, and disrupted using  $\text{N}_2$  cavitation at 1500 psi for 30 min. Following lysis, pellicle-bound plasma membrane sheets were separated from other cellular components by low speed sedimentation at 100 xg for 7 min, and washed three times with the lysis buffer, three times with 1 M  $\text{Na}_2\text{CO}_3$ , pH 11.4, and three more times with 1M KCl. The plasma membrane proteins were extracted in triplicate from the pellicles in 2% SDS, 62.5 mM Tris-HCl, and 5%  $\beta$ -mercaptoethanol at 100 °C for 5 min in a microwave oven (CEM Corporation, Matthews NC). Care was taken that all preparations were made in the same manner. Protein concentration was determined using an RCDC protein assay kit (Bio-Rad, Hercules CA).

Although we have made multiple analyses with all three pellicles, each of the three experiments reported here began with about 60 million cells, which provided a 1/6 aliquot for SEM and TEM characterization, 5 or 6 Western blots, and 6 (technical) replicate LC-MS/MS analyses.

### Western Blotting

Twenty-five micrograms of each pellicle enriched protein sample and 25  $\mu\text{g}$  of protein from a whole cell lysate were subjected to gel electrophoresis together on a 7.5% Bio-Rad Criterion precast gel and transferred to a PVDF membrane using the Bio-Rad Mini transblot electrophoretic transfer cell. The plasma membrane marker,  $\text{Na}^+\text{-K}^+$  ATPase ( $\alpha$ -subunit), was detected using mouse anti- $\text{Na}^+\text{-K}^+$  ATPase ( $\alpha$ -subunit) as the primary antibody and an alkaline phosphatase-conjugated goat anti-mouse IgG as the secondary antibody. Colorimetric detection was performed by incubating in BCIP®/NBT solution (Sigma-Aldrich, St. Louis MO). The protein bands were interrogated using ChemiDoc™ XRS+ System with Image Lab™ Software (Bio-Rad, Hercules CA).

### Sample preparation for scanning electron microscopy

The cells or the plasma membrane sheets were washed with 0.12 M Millonig's phosphate buffer, pH 7.3 (24), and fixed with 2% glutaraldehyde, followed by 1%  $\text{OsO}_4$ . Then the cells were dehydrated in a series of ethanol solutions and subjected to a critical point drying with  $\text{CO}_2$  using a Denton DCP-1 critical-point dryer (Denton Vacuum, LLC, Moorestown, NJ). The samples were coated with Au:Pd in a DV-503 Denton Vacuum evaporator (Denton Vacuum, LLC, Moorestown, NJ). SEM and TEM microscopy were performed on a Hitachi SU-70 Field Emission scanning electron microscope (Hitachi, Gaithersburg MD) and an Amray 1820 scanning electron microscope (AmrayInc, Bedford MA) was also used for SEM.

### Proteomic Analysis

For each type of pellicle, 90  $\mu\text{g}$  of proteins was precipitated with chloroform/methanol (28) to remove phospholipids and detergent. The protein pellets were resolubilized in 8M urea in 50 mM  $\text{NH}_4\text{HCO}_3$ , reduced by 20 mM DTT at 56 °C for 30 min and alkylated by

40mM iodoacetamide in the dark for 30 min. Lys-C digestion was performed in the presence of 8 M urea for 3 h at 37 °C, using a 1:50 enzyme/protein ratio. Trypsin cleavage was performed in 1.6 M urea for 16 h at 37 °C, using the enzyme/protein ratio of 1:25. Tryptic peptides were desalted using Pierce® C18 spin columns and subjected to HPLC-MS/MS analysis.

The HPLC-MS/MS analyses were carried out using a Shimadzu Prominent nanoHPLC (Shimadzu BioSciences, Columbia MD) interfaced to an LTQ-orbitrap XL (Thermo Fisher Scientific, San Jose CA). For each pellicle, six (technical) replicate injections were performed in order to maximize peptide identification from the complex mixtures. Three biological replicate experiments, from different batches of cell culture, were carried out in order to evaluate reproducibility of the entire enrichment procedure. Fifteen micrograms of the peptides extracted using each pellicle were injected to an Acclaim PepMap 300 C18 precolumn (Dionex, Sunnyvale CA) and desalted by 10% solvent A (97.5% H<sub>2</sub>O, 2.5% acetonitrile, 0.1% formic acid) for 10 min, using a flow rate of 10 µL/min. Following trapping, peptides were fractionated in a Zorbax 300SB-C18 (Agilent Technologies, Palo Alto CA) nanobore column (0.075 × 150 mm) with a linear gradient increasing from 10 to 60% solvent B (97.5% acetonitrile, 2.5% H<sub>2</sub>O, 0.1% formic acid) in 90 min, followed by another increase from 60% B to 85% B in 20 min. The fractionation flow rate was set at 300 nL/min. A 15 µm fused-silica PicoTip® (New Objective, Inc., Woburn, MA) was used as an emitter, interfaced with a Thermo nano-electrospray ionization (ESI) source (Thermo Fisher Scientific, San Jose CA). Electrospray parameters included a spray voltage of +2.0 kV, a capillary temperature of 275 °C and a tube lens voltage of 100 V. Precursor ions were measured in the orbitrap at a resolution of 30,000 at m/z 400. In each activation cycle, the nine most abundant precursor ions were fragmented by collisioninduced dissociation (CID) with normalized collision energy of 35; and the product ions were scanned in the LTQ at unit resolution. The peptide precursor ions were isolated within a 3 Da window for activation through 30 ms. Ions with unassigned or +1 charge states were excluded from selection for MS/MS. Dynamic exclusion was enabled to exclude precursor ions that were previously scanned within 3 min. Spectra were recorded using Xcalibur 2.0 software (Thermo Fisher Scientific, San Jose CA).

## Bioinformatics

RAW spectral files were subject to centroiding and mzXML reformatting using msconvert from the ProteoWizard project (29) and submitted to the PepArML meta-search engine (March 2012) (30) using the PepArML batch uploader. Tandem mass spectra were searched against the human reference proteome from the UniprotKnowledgeBase (March 2012) with enumerated isoforms. Carbamidomethylation was specified as a fixed modification on Cys, and oxidation of Met was allowed as a variable modification.

Peptide identifications from PepArML were filtered at 10% (spectral) FDR and a global parsimony analysis used to eliminate redundantly identified proteins. The global parsimony analysis ensures, in particular, that groups of equivalent proteins with identical peptide evidence are consistently represented by a specific protein from the group, even in different datasets. The (generalized) parsimony analysis applied here using an in-house tool requires that each retained protein be supported by at least two distinct peptides not shared with any other (retained) protein. This filtering criterion allows us to establish an upper-bound estimate of 1% on the protein falsediscovery-rate, presuming distinct peptide errors are independent. (See Supplementary Tables 2 and 3.)

Spectral counts for retained protein were determined from filtered peptide identifications, without adjustment for shared peptides or length of the protein sequence. As such, these spectral counts are only appropriate for comparison of protein abundance across samples



(pellicles) and should not be used to compare the abundance of different proteins within a sample. Protein (or protein group) spectral counts expressed as percentages are with respect to the total number of peptide identifications for the pellicles' samples. In-house software (SpectralCount v1.5) was used to compute spectral counts from PepArML peptide identifications.

Subcellular localization of identified proteins to the plasma membrane was determined by an in-house application of the map2slim script from the go-perl software package available from the Gene Ontology project, the Uniprot human Gene Ontology Annotation (GOA), and a specialized in-house defined GO Slim. Identified proteins were categorized as transmembrane based on the "Transmembrane" keyword annotations in UniProt or by the application of the webbased TMHMM2.0 tool (31) for predicting transmembrane helices from protein sequence.

A gene set enrichment analysis of pellicle unique proteins was performed with the functional analysis tool of Database for Annotation, Visualization and Integrated Discovery (DAVID) version 6.7 (32) using the UniProt accessions of proteins retained after the global parsimony analysis. Proteins observed only in a single pellicle's identifications were submitted as a gene list for DAVID analysis, with the list of all single-pellicle proteins used as the background. Cellular location terms from DAVID's GO Cellular Component FAT database were evaluated using Fisher's exact-test with the best hit and its *p*-value (uncorrected for multiple testing) reported.

## Results and Discussion

Fe<sub>3</sub>O<sub>4</sub> (magnetite) nanoparticles were synthesized and coated with Al<sub>2</sub>O<sub>3</sub> as described in the experimental section. A micrograph of a sample of these particles is shown in Figure 1, along with elemental analysis determined by EDX measurements. The diameter of the dry nanoparticles and the diameter of the aggregated nanoparticles in the buffered solution used to coat suspended cells were measured using SEM and TEM, and the zeta potential of the aggregates was measured using a particle analyzer. These are summarized in Table 1, along with physical properties determined by us for the commercial cationic nanoparticles comprising aluminosilicate, and a sample of Al<sub>2</sub>O<sub>3</sub>coated SiO<sub>2</sub> nanoparticles kindly provided by Prof. Donna Beer Stolz (10). A micrograph of these widely used particles is provided in Supplementary Figure 1, which shows a range of sizes between 20 and 100 nm and an average consistent with previous reports (10-12). The size of the synthetic Fe<sub>3</sub>O<sub>4</sub>particles was controlled to match the uniform size of the commercial particles and the lower range of the Al<sub>2</sub>O<sub>3</sub>coated SiO<sub>2</sub> particles. The Fe<sub>3</sub>O<sub>4</sub> core provides significantly increased density, which was expected to enhance differential centrifugation of coated plasma membrane fragments. Zhang *et al* (3) and Li *et al* (20) have previously reported construction of pellicles using cationic amino group coated magnetite nanoparticles with diameters of 200 and 10 nanometers, respectively. They focused their studies on magnetic field-based separations of pellicles, while we compare the high density property of magnetite with densities of conventionally used silica nanoparticles.

The three different nanoparticles were used to coat multiple myeloma cells in suspension and capped with polyacrylate. The coated cells were lysed by nitrogen cavitation (see Materials and Methods) and fragments of the pellicle-covered plasma membrane were isolated by low speed centrifugation. Figure 2 shows electron micrographs of multiple myeloma cells, cells coated with the three kinds of nanoparticles, coated cells cross-linked with poly acrylate and a piece of the pellicle coated plasma membrane produced with each of the three pellicles.

Pellicle-coated membrane fragments were washed as described in the experimental section, and pellicle-bound proteins were solubilized. The concentration of  $\text{Na}^+\text{-K}^+$  ATPase was assayed in each of the three isolates, relative to its presence in whole cell lysate, using Western blotting. These bands are shown in Figure 3. Significant enrichment of  $\text{Na}^+\text{-K}^+$  ATPase is revealed, measured spectroscopically as 33, 7 and 50 fold for the aluminosilicate particles,  $\text{Al}_2\text{O}_3$  coated  $\text{SiO}_2$  particles and  $\text{Al}_2\text{O}_3$  coated  $\text{Fe}_3\text{O}_4$  particles, respectively. The enrichment of this marker protein was also evaluated by spectral counting, also in Figure 3, which confirms the enrichment of  $\text{Na}^+\text{-K}^+$  ATPase observed by Western blotting. Spectral counts of a small number of other plasma membrane marker proteins are also provided.

The desired outcome of efforts to improve plasma membrane enrichment in this and other laboratories is to increase the number of peptide and protein identifications and quantifications made using high throughput LC-MS/MS technologies. In our case we expect to apply an optimized workflow to the qualitative and quantitative proteomic analyses of cells isolated from mouse blood. Previous workers using the pellicle technique (e.g., 14,22,23) have reported enrichments of individual markers, judged by Western blotting, that correlated poorly with overall proteomic identifications. In order to evaluate enrichment based on proteomic analysis in our experiments, the protein mixture recovered from each of the pellicles was digested with trypsin. Six replicate injections were made for LC-MS/MS analyses of each of the three tryptic peptide mixtures. We found peptide sampling to be saturated (33) after six injections. In Table 2 identifications of plasma membrane proteins are summarized as a percent of total protein identifications and can be compared to an analogous analysis of whole cell lysate. In this analysis the proportion of plasma membrane proteins in pellicle samples are enriched, with the pellicles providing 16% to 24% plasma membrane proteins compared to just 13% from the whole cell lysate. Lists of proteins and peptides identified in each of the pellicle samples and the whole cell lysate are provided in Supplementary Tables 2 and 3. Although the cellular localization annotations cannot be considered entirely reliable, the assignments in the Table were made consistently for all experiments, and thus can be compared. The most dense pellicle,  $\text{Al}_2\text{O}_3$  coated  $\text{Fe}_3\text{O}_4$ , provides the best enrichment (as a percent of total identifications) relative to the whole cell lysate control analysis. A similar trend was observed from multiple batches of cell culture (three biological replicates) shown in Supplementary Table 1, indicating good consistency and reproducibility of this technique.

Figure 4A shows the average spectral count assigned to plasma membrane proteins in each of three biological replicates as a percent of the total number of peptide identifications and again provides a comparison with the whole cell lysate control. The proportion of spectral counts for plasma membrane proteins ranges from 23 to 28%, compared to the control at 20%. Minimum and maximum values for the three (biological) replicates are shown as error-bars in the figure. With this small sample size ( $n=3$ ), it is difficult to conclude that the enrichment due to the aluminosilicate and  $\text{Al}_2\text{O}_3/\text{SiO}_2$  pellicles is statistically significant, but for the  $\text{Fe}_3\text{O}_4/\text{Al}_2\text{O}_3$  pellicles the enrichment is clear. The corresponding plot for the six technical replicates (Supplementary Figure 2) shows a clearer separation from the whole cell-lysate for all three pellicles.

All three pellicles show (Table 2, six technical-replicates) much stronger enrichment, compared to whole cell lysate, of proteins classified by UniProt annotation as transmembrane proteins, and also of transmembrane proteins as predicted by TMHMM2.0. This is hardly surprising, as the annotated and predicted transmembrane proteins are largely concordant. Enrichment of transmembrane proteins was further confirmed by spectral counting, as shown in Figure 4B (three biological replicates) and Supplementary Figure 2B (six technical replicates). It can be seen that enrichment in the pellicle experiments is 3 to 4 fold relative to whole cell lysate.

The possibility that different pellicles might preferentially enrich different sets of proteins was examined, given the rather striking difference in the enrichment of annotated plasma membrane proteins vs transmembrane proteins. A Venn diagram (Figure 5) illustrates the overlapping and unique plasma membrane proteins identified by the three types of pellicles. We stress that the global parsimony analysis used (see Methods) ensures that identified proteins can be reliably classified as overlapping or unique. The majority of proteins identified are common to all three experiments, and a smaller number of proteins were identified uniquely by each pellicle. A functional enrichment analysis of the proteins uniquely identified with each pellicle was made using GO FAT cellular component categories in the DAVID functional annotation tool. The background set comprised the three lists of pellicle-unique proteins. This analysis suggests that each set of pellicle-unique proteins has a distinct cellular origin in comparison to the other pellicles. The aluminosilicate particles appear to enrich basic proteins from the ribosome (Fisher's exact test  $p$ -value  $5.8 \times 10^{-4}$ ) and cytosol ( $p$ -value  $1.1 \times 10^{-2}$ ), while proteins uniquely associated with the  $\text{Al}_2\text{O}_3$  coated  $\text{Fe}_3\text{O}_4$  pellicle originate primarily from the plasma membrane ( $p$ -value  $9.8 \times 10^{-3}$ ). Unique proteins recovered by the  $\text{Al}_2\text{O}_3$  coated  $\text{SiO}_2$  pellicles do not show a significant bias in cellular localization, compared to the background set. The possibility of differential enrichment by different pellicles is intriguing and deserves additional study.

In summary, based on both protein identifications and spectral counts, the capability of the nanoparticle pellicles studied to provide enriched samples of plasma membrane proteins from suspended cells is real though limited. The enrichment provided by  $\text{Al}_2\text{O}_3$  coated  $\text{Fe}_3\text{O}_4$  particles trends higher than the other two studied, consistent with the hypothesis that higher density particles are more effective. Plasma membrane protein identifications and spectral counts determined as percentages of total proteins in the three pellicle samples (18-26%) are within the range of observations published by others for suspended cells (18-42%) (14,17,20,22). The comparison provided here, with a control analysis of whole cell lysate, indicates that improvements in the proportion of plasma membrane protein identifications and spectral counts are provided by using the pellicles. Enrichment of the more limited category of transmembrane proteins is found to be about three-fold greater than the control lysate, based on identifications and spectral counts, and the pellicle method seems well suited for this target group. Enrichments of individual protein markers (Western blotting and spectral counting) were found to correlate poorly with changes in the percentages of identifications and spectral counts of all plasma membrane proteins. Work is currently underway in our laboratory to evaluate the efficacy of pellicles constructed with nanowires, which offer multiple ionic contact points with the exterior of the plasma membrane.

## Supplementary Material

Refer to Web version on PubMed Central for supplementary material.

## Acknowledgments

The authors thank Professor Donna Beer Stolz (University of Pittsburg) for providing a sample of  $\text{Al}_2\text{O}_3$ -coated  $\text{SiO}_2$  nanoparticles. The authors thank Dr. Yan Wang, Director of Proteomic Core Facility, Maryland Pathogen Research Institute, University of Maryland, College Park, for advice with LC-MS/MS analysis, and Tim Mangel, Director of Laboratory for Biological Ultrastructure, University of Maryland, College Park for assisting with SEM processing. We acknowledge the support of the Maryland NanoCenter and its NispLab. The NispLab is supported in part by the National Science Foundation as an MRSEC Shared Experimental Facility."

The research reported here was supported by a grant from the National Institutes of Health, GM 021248. SBL also thanks the WCU program through the National Research Foundation of Korea funded by the Ministry of Education, Science and Technology, R31-2008-000-10071-0. WC acknowledges a Royal Thai Government Fellowship.



## References

1. Stevens TJ, Arkin IT. Do more complex organisms have a greater proportion of membrane proteins in their genomes? *Proteins:Structure, Function and Genetics*. 2000; 39:417–420.
2. Overington JP, Al-Lazikni B, Hopkins AL. How many drug targets are there? *NatureReviews/Drug Discovery*. 2006; 5:993–996.
3. Zhang W, Zhao C, Wang S, Fang C, Xu Y, Lu H, Yang P. Coating cells with cationic silica-magnetite nanocomposites for rapid purification of integral plasma membrane proteins. *Proteomics*. 2011; 11:3482–3490. [PubMed: 21751343]
4. Speers AE, Wu CC. Proteomics of integral membrane proteins—theory and application. *Chem. Rev.* 2007; 107:3687–3714. [PubMed: 17683161]
5. Shin BK, Wang H, Yim AM, LeNaour F, Brichory F, Jang JH, Zhao R, Puravs E, Tra J, Michael CW, Misek DE, Hanash SM. Global profiling of the cell surface proteome of cancer cells uncovers an abundance of proteins with chaperone function. *J. Biol. Chem.* 2003; 278:7607–7616.
6. Zhang H, Li XJ, Martin DB, Aebersold R. Identification and quantification of N-linked glycoproteins using hydrazide chemistry, stable isotope labeling and mass spectrometry. *Nat Biotechnology*. 2003; 21:660–666.
7. Zhao Y, Zhang W, Kho Y, Zhao Y. Proteomic Analysis of Integral Plasma Membrane Proteins. *Anal. Chem.* 2004; 76:1817–1823. [PubMed: 15053638]
8. Choksawangkarn W, Edwards N, Wang Y, Gutierrez P, Fenselau C. Comparative Study of Workflows Optimized for In-gel, In-solution, and On-filter Proteolysis in the Analysis of Plasma Membrane Proteins. *J Proteome Res.* 2012; 11:3030–3034. [PubMed: 22500775]
9. Chaney LK, Jacobson BS. Coating cells with colloidal silica for high yield isolation of plasma membrane sheets and identification of transmembrane proteins. *J. Biol. Chem.* 1983; 258:10062–10072. [PubMed: 6309765]
10. Stolz DB, Jacobson BS. Examination of transcellular membrane protein polarity of bovine aortic endothelial cells in vitro using the cationic colloidal silica microbead membraneisolation procedure. *J Cell Science.* 1992; 103(Pt 1):39–51. [PubMed: 1331135]
11. Stolz DB, Ross MA, Salem HM, Mars WM, Michalopoulos GK, Enomoto K. Cationic Colloidal Silica Membrane Perturbation as a Means of Examining Changes at the Sinusoidal Surface During Liver Regeneration. *Amer J Pathology.* 1999; 155:1487–1498.
12. Robinson JM, Ackerman W. E. t. Tewari AK, Kniss DA, Vandre DD. Isolation of highly enriched apical plasma membranes of the placental syncytiotrophoblast. *Anal Biochem.* 2009; 387:87–94. [PubMed: 19454249]
13. Harvey S, Zhang Y, Landry F, Miller C, Smith JW. Insights into a plasma membrane signature. *Physiol Genomics.* 2001; 5:129–136. [PubMed: 11285366]
14. Rahbar AM, Fenselau C. Integration of Jacobson's pellicle method into proteomic strategies for plasma membrane proteins. *J Proteome Res.* 2004; 3:1267–1277. [PubMed: 15595737]
15. Rahbar AM, Fenselau C. Unbiased examination of changes in plasma membrane proteins in drug resistant cancer cells. *J Proteome Res.* 2005; 4:2148–2153. [PubMed: 16335961]
16. Li X, Xie C, Cao J, He Q, Cao R, Lin Y, Jin Q, Chen P, Wang X, Liang S. An in vivo membrane density perturbation strategy for identification of liver sinusoidal surface proteome accessible from the vasculature. *J Proteome Res.* 2009; 8:123–132. [PubMed: 19053532]
17. Li X, Jin Q, Cao J, Xie C, Cao R, Liu Z, Xiong J, Li J, Yang X, Chen P, Liang S. Evaluation of two cell surface modification methods for proteomic analysis of plasma membrane from isolated mouse hepatocytes. *Biochim Biophys Acta.* 2009; 1794:32–41. [PubMed: 18707032]
18. Leduc-Nadeau A, Lahjouji K, Bissonnette P, Lapointe JY, Bichet DG. Elaboration of a novel technique for purification of plasma membranes from *Xenopus laevis* oocytes. *Am J Physiol Cell Physiol.* 2007; 292:C1132–C1136. [PubMed: 17079335]
19. Jacobson BS, Stolz DB, Schnitzer JE. Identification of endothelial cell-surface proteins as targets for diagnosis and treatment of disease. *Nature Med.* 1996; 2:482–484. [PubMed: 8597963]
20. Li X, Jia X, Xie C, Lin Y, Cao R, He Q, Chen P, Wang X, Liang S. Development of cationic colloidal silica-coated magnetic nanospheres for highly selective and rapid enrichment of plasma

- membrane fractions for proteomics analysis. *Biotechnol Appl Biochem*. 2009; 54:213–220. [PubMed: 19860738]
21. Durr E, Yu J, Krasinska KM, Carver LA, Yates JR, Testa JE, Oh P, Schnitzer JE. Direct proteomic mapping of the lung microvascular endothelial cell surface in vivo and in cell culture. *Nature Biotechnol*. 2004; 22:985–992. [PubMed: 15258593]
22. Prior MJ, Larance M, Lawrence RT, Soul J, Humphrey S, Burchfield J, Kistler C, Davey JR, La-Borde PJ, Buckley M, Kanazawa H, Parton RG, Guilhaus M, James DE. Quantitative proteomic analysis of the adipocyte plasma membrane. *J Proteome Res*. 2011; 10:4970–4982. [PubMed: 21928809]
23. Mathias RA, Chen YS, Goode RJ, Kapp EA, Mathivanan S, Moritz RL, Zhu HJ, Simpson RJ. Tandem application of cationic colloidal silica and Triton X-114 for plasma membrane protein isolation and purification: towards developing an MDCK protein database. *Proteomics*. 2011; 11:1238–1253. [PubMed: 21337516]
24. Vandre DD, Ackerman WD, Tewari A, Kniss DA, Robinson JM. A placental sub-proteome: the apical plasma membrane of the syncytiotrophoblast. *Placenta*. 2012; 33:207–213. [PubMed: 22222045]
25. Arjunan S, Reinartz M, Emde B, Zanger K, Schrader J. Limitations of the colloidal silica method in mapping the endothelial plasma membrane proteome of the mouse heart. *Cell Biochem Biophys*. 2009; 53:135–143. [PubMed: 19184541]
26. Jang JH, Hanash S. Profiling the cell surface proteome. *Proteomics*. 2003; 3:1947–1954. [PubMed: 14625857]
27. Bai X, Son SJ, Zhang S, Liu W, Frank JA, Venkatesan T, Lee SB. Synthesis of superparamagnetic nanotubes as MRI contrast agents and for cell labeling. *Nanomedicine*. 2008; 3:163–166. [PubMed: 18373423]
28. Wessel D, Flugge UI. A method for the quantitative recovery of protein in dilute solution in the presence of detergents and lipids. *Anal Biochem*. 1984; 138(1):141–143. [PubMed: 6731838]
29. Kessner D, Chambers M, Burke R, Agus D, Mallick P. ProteoWizard: Open Source Software for Rapid Proteomics Tools Development. *Bioinformatics*. 2008; 24(21):2534–2536. [PubMed: 18606607]
30. Edwards N, Wu X, Tseng TW. An unsupervised, model-free, machine-learning combiner for peptide identifications from tandem mass spectra. *Clinical Proteomics*. 2009; 5:23–36.
31. Krogh A, Larsson B, von Heijne G, Sonnhammer ELL. Predicting transmembrane protein topology with a hidden Markov model: Application to complete genomes. *Journal of Molecular Biology*. 2001; 305(3):567–580. [PubMed: 11152613]
32. Huang W, Sherman BT, Lempicki RA. Systematic and integrative analysis of large gene lists using DAVID bioinformatics resources. *Nat Protoc*. 2009; 4:44–57. [PubMed: 19131956]
33. Liu H, Sadygov RG, Yates JR. A model for random sampling and estimation of relative protein abundance in shotgun proteomics. *Anal. Chem*. 2004; 76:4193–4201. [PubMed: 15253663]

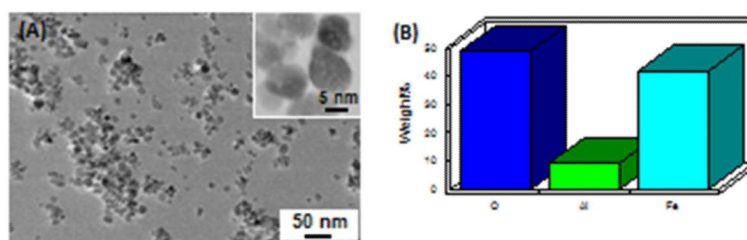
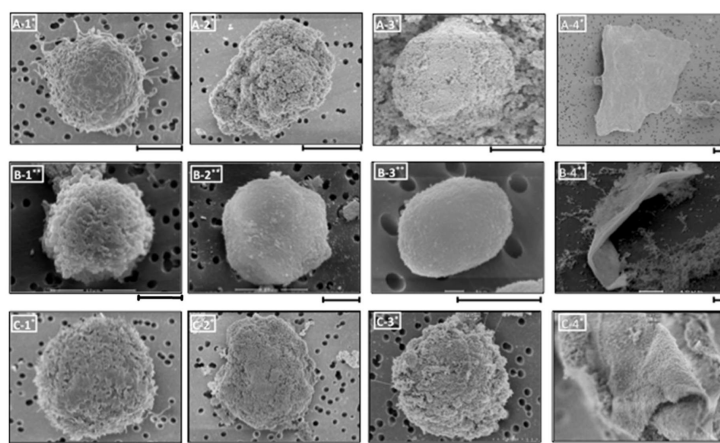


**Figure 1.**  
A) TEM micrograph of alumina-coated iron oxide nanoparticles. (B) Elemental composition of alumina-coated iron oxide nanoparticles.



\* micrographs were taken with an Hitachi SU-70 field emission scanning electron microscope.

\*\* micrographs were taken with an Amray 1820 scanning electron microscope.

**Figure2.**

Micrographs of : (A-1 to A-4) multiple myeloma cell, the cell coated with  $\text{Fe}_3\text{O}_4/\text{Al}_2\text{O}_3$  nanoparticle, polyacrylic acid cross-linked  $\text{Fe}_3\text{O}_4/\text{Al}_2\text{O}_3$  coated cell, and a fragment of the pellicle-coated plasma membrane ; (B-1 to B-4) intact cell, the cell coated with aluminosilicate nanoparticle, polyacrylic acid cross-linked cell, and a pellicle-coated plasma membrane sheet ; (C-1 to C-4) control cell,  $\text{SiO}_2/\text{Al}_2\text{O}_3$  coated cell, polyacrylic acid cross-linked cell, and a plasma membrane-pellicle. Scale bars indicates 5  $\mu\text{m}$  in length.

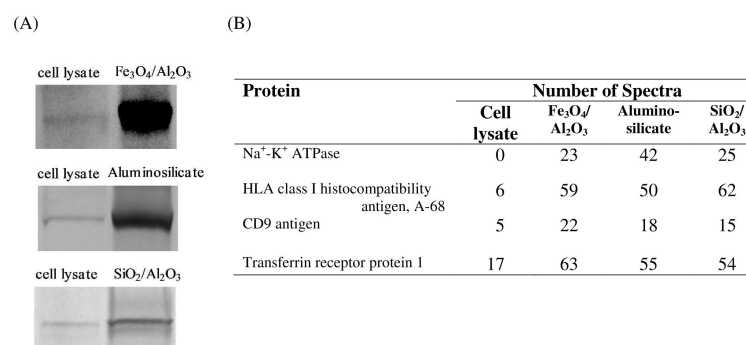


**Figure 3.** Analysis of an abundance of plasma membrane protein markers by (A) Western Blotting of Na<sup>+</sup>-K<sup>+</sup> ATPase and (B) Spectral counts for Na<sup>+</sup>-K<sup>+</sup> ATPase and other plasma membrane protein markers.



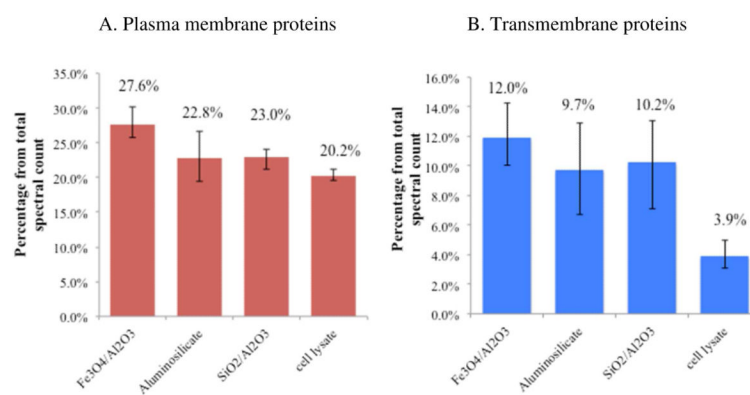


**Figure 4.** Spectral counts from three biological replicates of (A) plasma membrane proteins as a percent of total spectral counts; and (B) transmembrane proteins as a percent of total spectral counts. Error bars indicate range of observed values.

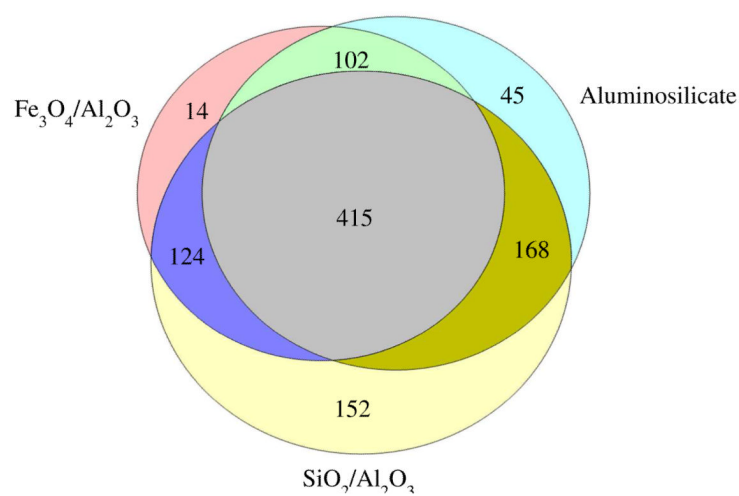


**Figure 5.** Number of common, shared, and unique protein identifications for  $\text{Al}_2\text{O}_3$  coated  $\text{Fe}_3\text{O}_4$ , aluminosilicate, and  $\text{Al}_2\text{O}_3$  coated  $\text{SiO}_2$  nanoparticles.

**Table 1**

Properties of the nanoparticles studied

Nanoparticles	Diameter (nm)	Density (g/mL)	Size in solution (nm)	Cationic group	Zeta potential (mV)
Fe <sub>3</sub> O <sub>4</sub> /Al <sub>2</sub> O <sub>3</sub>	17±6	5.17 <sup>*</sup>	99±55	Al <sub>2</sub> O <sub>3</sub>	64±3
Aluminosilicate	18±5	1.23 <sup>**</sup>	55±2	Al <sub>2</sub> O <sub>3</sub>	86±2
SiO <sub>2</sub> /Al <sub>2</sub> O <sub>3</sub>	20-100	2.65 <sup>*</sup>	31±6	Al <sub>2</sub> O <sub>3</sub>	50±6

<sup>\*</sup> Bulk density of the core

<sup>\*\*</sup> Density provided by Sigma-Aldrich

**Table 2**

Proteomic analysis of plasma membrane (PM) and transmembrane (TM) protein enrichment by three pellicles. Average % (standard deviation) of six technical-replicates.

Nanoparticle	Distinct Proteins	...with GOA Annotation	Average % Annot. PM*	Average % Annot. TM#	Average % Pred.TM##
Fe <sub>3</sub> O <sub>4</sub> /Al <sub>2</sub> O <sub>3</sub>	341	311	23.6 (0.5)	13.9 (0.7)	12.4 (0.7)
Aluminosilicate	381	337	18.5 (0.3)	13.0 (0.4)	12.3 (0.4)
SiO <sub>2</sub> /Al <sub>2</sub> O <sub>3</sub>	530	435	16.7 (1.0)	10.6 (0.5)	10.6 (0.4)
Whole cell lysate	658	589	13.1 (0.6)	4.6 (0.2)	4.5 (0.5)